

Intrinsic ferroelectric instability in $\text{Pb}(\text{In}_{1/2}\text{Nb}_{1/2})\text{O}_3$ revealed by changing B-site randomness: Inelastic x-ray scattering study

Kenji Ohwada,^{1,2,*} Kazuma Hirota,³ Hikaru Terauchi,⁴ Tatsuo Fukuda,¹ Satoshi Tsutsui,⁵ Alfred Q. R. Baron,^{6,5} Jun'ichiro Mizuki,^{1,2} Hidehiro Ohwa,⁷ and Naohiko Yasuda⁷

¹Quantum Beam Science Directorate (in SPring-8), Japan Atomic Energy Agency, 1-1-1 Kouto, Sayo-cho, Sayo-gun, Hyogo 679-5148, Japan

²CREST, Japan Science and Technology Agency (JST), Kawaguchi, Saitama 332-0012, Japan

³Neutron Science Laboratory, Institute for Solid State Physics, The University of Tokyo, 106-1 Shirakata, Tokai, Ibaraki 319-1106, Japan

⁴Advanced Research Center of Science, School of Science, Kwansai Gakuin University, Sanda, Hyogo 669-1337, Japan

⁵Japan Synchrotron Radiation Research Institute (SPring-8), 1-1-1 Kouto, Sayo-cho, Sayo-gun, Hyogo 679-5198, Japan

⁶Materials Dynamics Laboratory, RIKEN SPring-8 Center, 1-1-1 Kouto, Sayo-cho, Sayo-gun, Hyogo 679-5148, Japan

⁷Electrical and Electric Engineering Department, School of Engineering, Gifu University, Gifu 501-1193, Japan

(Received 28 December 2007; revised manuscript received 4 March 2008; published 28 March 2008)

Antiferroelectric (AFE), ferroelectric (FE), or relaxor states can appear in $\text{Pb}(\text{In}_{1/2}\text{Nb}_{1/2})\text{O}_3$ (PIN) depending on the perovskite B-site randomness. We studied the effects of this randomness on the dynamics of PIN by high resolution inelastic x-ray scattering using ordered PIN (AFE) and disordered PIN (relaxor) single crystals. We have found a clear softening of a transverse optic mode at the Γ point in both samples, indicating a robust and intrinsic ferroelectric dynamical correlation regardless of the actual ground state. We believe that the correlation results in a FE instability mode, which gives yield to the FE and relaxor states. We interpret that AFE is stabilized only when In and Nb ions are spatially ordered enough to overwhelm the FE instability. As the B-site randomness becomes larger, AFE is suppressed and the hidden FE state starts appearing. Ultimately, the randomness begins to predominate over the development of FE regions and blocks a long range FE order, which we believe yields polar nanoregions resulting in relaxor behaviors.

DOI: [10.1103/PhysRevB.77.094136](https://doi.org/10.1103/PhysRevB.77.094136)

PACS number(s): 61.05.C-, 63.20.-e, 77.80.-e

I. INTRODUCTION

Relaxors are characterized by a number of unusual properties, many of which are not fully understood. The dielectric constant $\epsilon(T)$ exhibits a large and broad peak around T_{max} , which is usually near room temperature (RT). ϵ and T_{max} strongly depend on the frequency of the external field, which indicates a relaxation process with multiple time scales. For nearly half a century since the discovery of relaxors,^{1,2} much attention has been paid to lead-based-perovskite relaxors because they often show colossal dielectric and piezoelectric responses, which is appealing for industrial applications. Despite long and intensive research, however, arguments about the intrinsic mechanism for unusual properties in lead-based relaxors are still unsettled. This is mainly because we have to deal with the nanoscale randomness intrinsic to the relaxors.

The lead-based relaxors have a $\text{Pb}(\text{B}'\text{B}'')\text{O}_3$ complex-perovskite structure, where two different ions occupy the B site stoichiometrically to conserve the average charge of 4+, e.g., the prototypical relaxor $\text{Pb}(\text{Mg}_{1/3}^{2+}\text{Nb}_{2/3}^{5+})\text{O}_3$ (PMN).¹⁻³ Since a 1:2 order (cell tripling) has not been observed in the relaxors, such a 1:2-type relaxor seems to have a kind of frustration at the B site. In a simple consideration, the 1:1 order (cell doubling) is favorable for smaller strain, while the 1:2 order is required for the charge neutrality. As a result, the B site becomes inevitably random. There is another type of relaxor such as $\text{Pb}(\text{In}_{1/2}\text{Nb}_{1/2})\text{O}_3$ (PIN),⁴ which does not have frustration and the B-site randomness might be controlled. Indeed, the B-site randomness of PIN is controllable by heat treatment, e.g., In and Nb are 1:1 ordered along the

111 direction when PIN is annealed, while disordered when it is quenched. PIN with the 1:1 ordered B site transforms into an antiferroelectric (AFE) state.⁵ PIN with a partially ordered B site is ferroelectric (FE).⁶ PIN with a strong B-site randomness becomes a relaxor.⁵ Thus, the B-site randomness is an essential condition for the relaxor state.

It is generally accepted that the relaxor properties are associated with the so-called polar nanoregions (PNRs), which were originally proposed by Burns and Dacol^{7,8} through measurements of the refraction indices $n(T)$ of PMN⁷ and $\text{Pb}(\text{Zn}_{1/3}\text{Nb}_{2/3})\text{O}_3$ (PZN).⁷ They found that $n(T)$ deviates from an ordinary linear temperature dependence below a characteristic temperature $T_d \sim 600$ K, which is much higher than $T_{max} \sim 300$ K. They proposed a model that randomly oriented, nanoscale polar regions start appearing locally in the paraelectric matrix below the Burns temperature T_d , which gives rise to the unexpected deviation of $n(T)$ without affecting macroscopic dielectric properties and grow with decreasing temperature.

It is well known that PNRs give diffuse scattering around a fundamental Bragg position. In the case of PMN, the diffuse intensities were seemingly unrelated to the amplitude of a condensed soft transverse-optic (TO) mode,^{9,10} which was originally pointed out by Vakhrushev and co-workers.^{11,12} To study the inconsistency, Hirota *et al.*¹³ revisited PMN by neutron diffuse and inelastic scatterings. They reached a conclusion that the diffuse scattering intensities are not only from the condensed soft TO mode but also from a uniform phase shift of PNRs against the surrounding paraelectric matrix. The uniform phase shift sets in when the soft TO mode

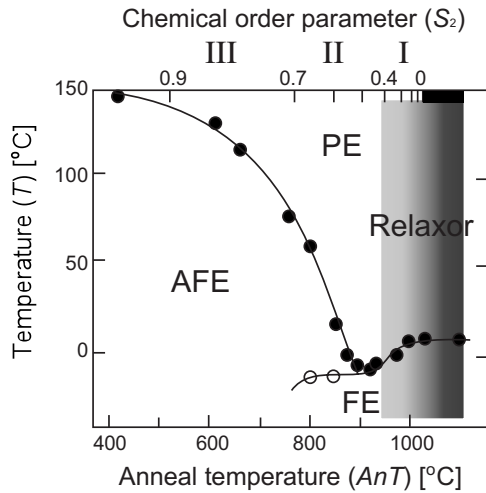


FIG. 1. S_2 -AnT- T phase diagram of PIN (Ref. 4).

is condensed and breaks the center of mass condition kept for phonons. Concerning this concept, Wakimoto *et al.*¹⁴ revealed a mode coupling between TA and the soft TO modes in PMN, which provides a mechanism for uniform phase shift. After their work, the importance of mode couplings in relaxors has been reported by some groups.¹⁵⁻¹⁷

We now know that the B-site randomness plays an essential role in the relaxor properties and that phonon behaviors are important to the relaxors as well. How does the B-site randomness contribute to the instability of phonon modes? For solving this problem, we have chosen PIN, where the B-site randomness can be controlled by heat treatment. Figure 1 shows the S_2 -AnT- T phase diagram of PIN,^{4,18} where S_2 is the chemical order parameter⁵ at the B site and AnT is the annealing temperature. The ground state of PIN strongly depends on S_2 , i.e., AFE for $S_2 \geq 0.7$ (ordered PIN or O-PIN), FE for $0.4 \leq S_2 \leq 0.7$, and relaxor for $S_2 \leq 0.4$ (disordered PIN or D-PIN).

Until recently, only an inelastic neutron scattering (INS) had been able to measure the phonon dispersions. INS requires large 1 cc-class crystal for precise measurements of the phonons. However, it is difficult to grow a large enough PIN single crystal. Moreover, indium contained has a large neutron absorption coefficient. The situation has been changed by the appearance of the third generation synchrotron light sources, which facilitate high resolution (\sim meV) inelastic x-ray scattering (IXS) with high photon flux and $\sim 100 \mu\text{m}^2$ sized small beam. Thus the IXS technique has become another probe for the phonon-dispersion measurements. We therefore employed a high resolution IXS technique to study the structural dynamics of PIN.

II. EXPERIMENT

A. Sample preparation

Single crystals of PIN were grown by the flux method from $\text{PbO-In}_2\text{O}_3\text{-Nb}_2\text{O}_5$.⁶ The mixture in a platinum crucible was heated up to 1000 °C and held at this soak temperature for 5 h, then the melt was cooled to 950 °C at a rate of

3 K/h down to 800 °C at a rate of 5 K/h, and finally down to RT at a rate of 100 K/h. Typical size of the as-grown crystals were 1–2 mm and yellow in color. O-PIN was obtained by 20 h annealing at 650 °C, while D-PIN was obtained by a quenching from 900 °C using liquid nitrogen. The temperature dependences of the dielectric constant of O-PIN and D-PIN show AFE and relaxor behaviors, respectively, which are the average information within the bulk.

For IXS measurements, the PIN samples were cut for providing a $\{100\}$ plane and etched for eliminating the mechanical strain. Note that x ray used for scattering experiments usually have the penetration length of 1–100 μm , which depends on the wavelength and the sample studied. We define the region where x-rays penetrate as “skin,” which should be distinguished from nanometer-scale “surface.” Since there is a possibility that the state of the skin region is different from the bulk one,^{18,19} we confirmed the state of the prepared skin regions by x-ray scattering. We used a Mo $K\alpha$ radiation with the x-ray power of 55 kV \times 280 mA, which is monochromatized by a PG(002) reflection. The energy of the Mo $K\alpha$ radiation (17.5 keV) is close to that used in the IXS measurement (21.7 keV); thus, the skin thickness should be similar to each other.

Figure 2 shows the results of mesh scans in the H0L zone for (a) O-PIN and (b) D-PIN. The $\frac{1}{4}0\frac{1}{4}$ superlattice spots and no diffuse scattering were observed in the O-PIN crystal, as shown in Fig. 2(a). It means that the state of the prepared O-PIN is unambiguously a single phase of AFE.^{18,20} On the other hand, a strong diffuse scattering around the Bragg position and no superlattice spot were observed in the D-PIN crystal, as shown in Fig. 2(b), indicating that the state of the prepared D-PIN is a single phase of relaxor.^{18,21}

B. High resolution inelastic x-ray scattering

The phonon measurement was carried out using the high resolution IXS spectrometer at BL35XU of SPring-8.²² Data were collected using the Si (11 11 11) reflection at 21.747 keV, which provides an overall resolution of 1.6–1.8 meV depending on the analyzer crystal. Among all operating IXS facilities, BL35XU is uniquely well appointed for phonon measurements having a two dimensional analyzer array. The use of 12, 4 (horizontal) \times 3 (vertical), analyzer crystals, placed with 120 mm spacing at 9.8 m on the two-theta arm (horizontal scattering plane), and 12 independent detectors (room temperature CdZnTe chips, dark count rates $< \sim 0.001$ Hz) allows a collection of 12 momentum transfers simultaneously. This greatly facilitates data collection for both longitudinal and transverse modes when all four (three) analyzers can be placed along a common symmetry direction.²³ The full 95 mm diameter of each analyzer crystal was used to get a maximum count rate, so the momentum resolution was $\sim 0.1 \text{ \AA}^{-1}$ full width at half maximum (FWHM) at Si (11 11 11). The beam size at the sample was about $64 \times 70 \mu\text{m}^2$ (vertical \times horizontal) FWHM for Si (11 11 11). For all the works, a slit was placed before the sample to insure a proper alignment so that the beam was onto the sample and into the center of the spectrometer. The measured spectra were normalized using the beam intensity monitored at the downstream of this slit.

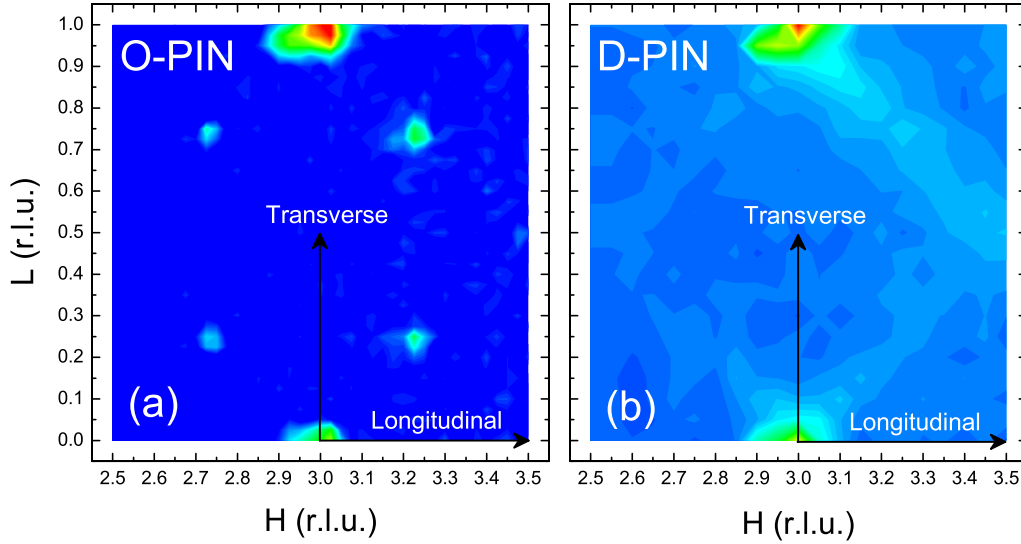


FIG. 2. (Color online) Mesh scan results of (a) O-PIN and (b) D-PIN. $\frac{\hbar}{4}0\frac{L}{4}$ superlattice spots for O-PIN and a strong, butterfly-shaped diffuse scattering for D-PIN were observed.

In the present experiment, the reciprocal lattice of each sample was set using a pseudo-cubic unit cell. We have measured transverse and longitudinal modes around the 3 0 0 positions. The scanning paths in a momentum space are shown in Fig. 2 by black arrows. All data were taken at room temperature.

III. EXPERIMENTAL RESULTS

A. Analysis of the inelastic spectrum

Figure 3 shows inelastic profiles of the transverse modes for O-PIN and D-PIN. The asymmetry of the intensity in the x-ray-energy gain ($E < 0$) and loss ($E > 0$) sides is due to the Bose factor. As shown in the panels of data at the zone boundary, the first peak around 6 meV is from the transverse-acoustic (TA) mode, while a broad peak around 15 meV is from the TO mode.

Each profile of the observed phonon modes is simply analyzed by a linear combination of damped-harmonic-oscillator (DHO) formulas.^{24,25} The response function for the DHO is written as

$$F_i(\omega) = \frac{\omega}{1 - e^{-\hbar\omega/kT}} \frac{\Gamma_i}{(\omega^2 - \omega_i^2)^2 + \omega^2\Gamma_i^2}, \quad (1)$$

where the phonon energy $\hbar\omega_i$ ($i=TA, TO, LA, LO1,$ and $LO2, L=longitudinal$) and the frequency-independent damping constant Γ_i (peak FWHM). The first factor in Eq. (1) is called the detailed balance factor. The equation describes energy loss process as well as energy gain process. An elastic scattering is described by the delta function $\delta(\omega)$. Finally, the fitting function $I(\omega)$ is defined by considering the resolution function $R(\omega)$ of each analyzer as

$$I(\omega) = \left(A \times \delta(\omega) + \sum_i B \times F_i(\omega) \right) * R, \quad (2)$$

where the operator “*” means a convolution. A and B are proportional coefficients for the present fitting and they are

proportional to the elastic component and dynamical structure factor, respectively. The resolution function $R(\omega)$ of each analyzer is experimentally determined. Mode coupling between acoustic and optic modes is not considered. The fitting results are shown in Fig. 3.

B. Intrinsic ferroelectric instability

Figure 4 shows the phonon dispersions of O-PIN and D-PIN. The transverse modes of O-PIN and D-PIN are displayed in Figs. 4(a) and 4(b) and the longitudinal modes are displayed in Figs. 4(c) and 4(d), respectively. The Γ point (3 0 0 position) is not accessible because of an elastic scattering. The solid lines drawn through the data are guides to the eye for making comparison between O-PIN and D-PIN. Note that the full energy scale for the transverse modes is different from that of the longitudinal modes.

The overall picture of the dispersions of O-PIN up to 30 meV is similar to that of D-PIN, e.g., the TA and LA modes almost degenerate, the energy of the TO mode is slightly higher than that of the LO1 mode, and the LO2 modes show a large softening toward the Γ -point as much as 12 meV. What particularly important in Fig. 4 is that the TO modes, which are ferroelectric modes, of both the samples show a large softening toward the Γ point of 6 meV. The result implies that a strong FE dynamical correlation exists not only in the ferroelectric relaxor D-PIN but also in the antiferroelectric O-PIN. Although we have not studied a possible condensation of the soft mode, we believe that the mode is unstable toward FE over a wide S2 range because the FE state is induced by a slight introduction of the B-site randomness.

C. Phonon folding in O-PIN

We have found that the observed LA branch of O-PIN strays out of the estimated LA branch [see the gray curve in

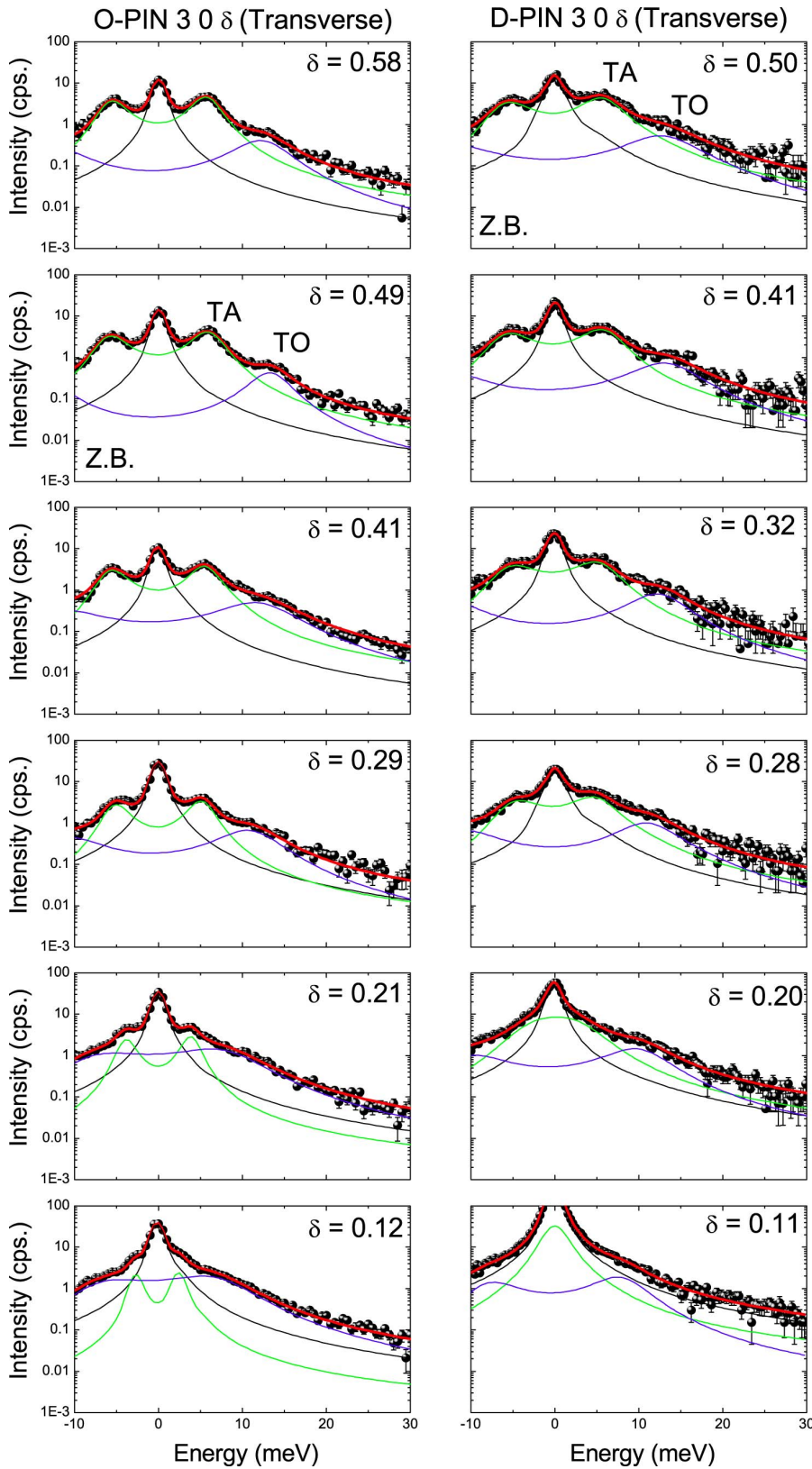


FIG. 3. (Color online) IXS profiles of transverse modes for O-PIN and D-PIN and fits with Eq. (2) using a least-squares method. The fitting results are shown by a red solid line. The components of the calculated profile are also shown by black (elastic), green (TA mode), and blue (TO mode) solid lines.

Fig. 5(a)]. We estimated that the LA branch of O-PIN is the same as that of LA of D-PIN. Since, as seen in Fig. 4, the TA branches of both the samples are almost same, and the LA and TA modes of D-PIN almost degenerate. We also show the inelastic profiles of the longitudinal modes of O-PIN and

D-PIN [see Figs. 5(b) and 5(c)]. The dotted lines are for a guide to the eyes. One can clearly see that the lowest branch of O-PIN (LA) shows a flat dispersion.

To explain such a flat dispersion toward the Γ point, we need to take a folding mode into account. The dotted curves

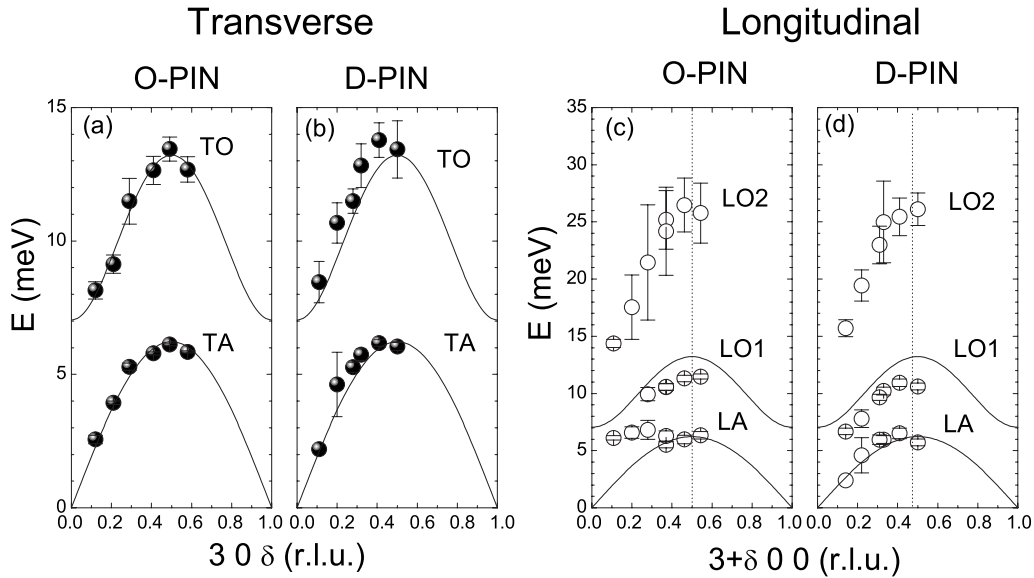


FIG. 4. Phonon dispersions of transverse modes of (a) O-PIN and (b) D-PIN and longitudinal modes of (c) O-PIN and (d) D-PIN. The solid and open circles represent the transverse and longitudinal modes, respectively. Two solid curves in each figure are guides to the eye with the aim of comparing O-PIN and D-PIN. Note that the full energy scale for the transverse modes is different from that of the longitudinal modes.

drawn in Fig. 5(a) are folded branches for $4a \times 4c$ unit cell for guides to the eye. The folding mode well explains the peak structure around $\delta=0.25$. The LA mode around $\delta=0.25$ and 0.5 are not observable near $E=0$ because no superlattice Bragg peaks exist at these momentum transfers. The scattering amplitude of the acoustic mode is proportional to the static structure factor (the square root of the

corresponding Bragg intensity). There is no evidence for the folding of LO1 and LO2 modes in the present results. We mention that we scanned around some $\frac{1}{4}0\frac{1}{4}$ superlattice spots but observed no acoustic mode because superlattice intensities are 10^2-10^3 times weaker than those of fundamental Bragg spots.

IV. DISCUSSION

A. Effect of the B-site randomness to the intrinsic ferroelectric instability

We have found clear softening of the TO modes near the Γ point in both the samples, O-PIN and D-PIN, as shown in Figs. 4(a) and 4(b). It is known that the softening trend of the TO modes toward the Γ point exists in a conventional relaxor ferroelectrics such as PMN⁹ and PZN.²⁶ The existence of the ferroelectric instability in antiferroelectric O-PIN is almost exactly the same way as in the relaxor D-PIN. It is significant for considering the origin of relaxor behavior in the lead-based-perovskite materials. The present results for PIN indicate that the ferroelectric instability intrinsically exists regardless of the ground state, in other words, the ferroelectric instability is independent of the B-site randomness.

How does the B-site randomness ($=S_2$) generate a relaxor state? We suppose that an antiferroelectric instability coexists with the ferroelectric instability in PIN because the AFE state appears in O-PIN. The antiferroelectric instability, however, has not been observed along the Γ -to-X zone studied in the present experiment. This is presumably because the phonon branches from the AFE superlattice peaks are too weak to be observable in the present IXS measurements, as mentioned in Sec. III C.

Based on the experimental facts and the above supposition, we suggest the following scenario concerning the phase

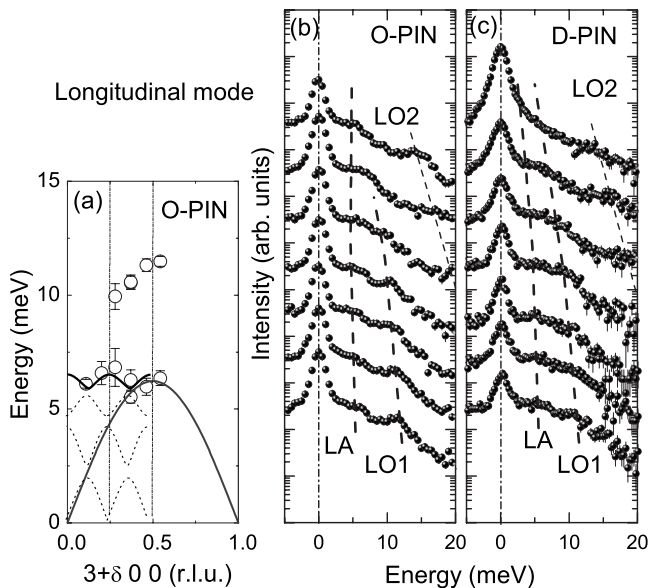


FIG. 5. (a) Longitudinal phonon modes of O-PIN. Folded branches are estimated as shown by dotted and solid curves. A dark gray curve represents the estimated LA dispersion, which is the same as that of LA of D-PIN. The inelastic profiles of the longitudinal modes of (b) O-PIN and (c) D-PIN are shown. The dotted lines are for a guide to the eyes.

transitions of PIN as the B-site randomness is increased (S_2 is decreased): The AFE state is stabilized when In and Nb ions are spatially ordered, overwhelming the FE instability. The hidden FE state appears as the B-site randomness becomes stronger and suppresses the AFE instability. Short-wavelength phonons (the AFE instability) might be easily affected by a randomness rather than long-wavelength phonons (the FE instability). Ultimately, the randomness competes with the development of FE regions and blocks a long range FE order. We believe that it gives yield to PNRs, resulting in relaxor behavior. Thus, the B-site randomness in PIN suppresses the AFE instability and enhances the FE instability, while blocking a long range FE order.

B. A-site off-centerness and antiferroelectric instabilities

In Sec. IV A, we have speculated that an antiferroelectric instability coexists with the ferroelectric instability in PIN. The coexistence of the instabilities will be predicted by considering another important structural character in the lead-based perovskite relaxor in addition to the B-site randomness. It has been revealed by precise structural analyses that the lead ion at the A site is strongly off-centered in relaxors such as PMN²⁷ and PZN.²⁸ Recent atomic pair distribution function method analysis of Yoneda *et al.*²⁹ on O-PIN and D-PIN also presented that the local environments of both the samples are quite similar, where the lead ions are strongly off-center. A conventional x-ray diffraction experiment of O-PIN performed at BL14B1 of SPring-8 (not shown) also suggests a large displacement of the lead ions. Let us call this behavior as “A-site off-centerness.” The structure analysis of the D-PIN shows the amount of the displacement of the lead ion to be about 0.3 Å.³⁰

Surprisingly, the A-site off-centerness is inherent to the lead-based AFE materials having a simple-perovskite structure such as PbZrO₃ (PZ)³¹ and PbHfO₃,³² while no A-site off-centerness is found in a prototypical FE material PbTiO₃ (PT).^{31–33} The relation between the A-site off-centerness and the AFE instability is understood in terms of chemical bonding. The off-centerness of the lead ion at the A site induces a covalent bonding between Pb 6*p* and the nearest neighbor O 2*p* states,³⁴ which will drive a lattice instability. Such a covalent bonding is clearly observed by a recent structural analysis.³¹ Actually, a first-principles study of antiferroelectric PZ³⁵ reproduces a coexistence of the FE instability with the AFE instability, e.g., an instability at the Γ point (zone center) and that at the M or R point (zone boundary). We therefore believe that there intrinsically exists a competition between the FE and the AFE instabilities inside the lead-based perovskite relaxor having the A-site off-centerness. Is such a coexistence of several kinds of lattice instabilities really necessary for generating a relaxor state? This might be an essential problem of relaxors.

We now also speculate that the B-site randomness controls a balance among several kinds of instabilities and finally chooses the FE instability but blocks a long range FE order.

C. Waterfall-like anomaly in PIN

Figure 6 shows the momentum dependence of the line width of the TO modes normalized by the mode energy. The

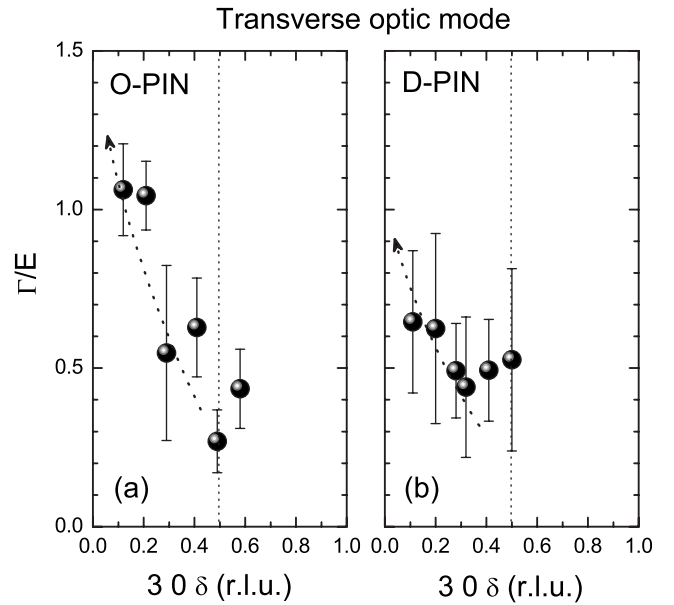


FIG. 6. Normalized line widths (Γ/E) of the transverse optic mode of (a) O-PIN and (b) D-PIN. A trend of the overdamping toward the Γ point (waterfall-like behavior) is seen in both O-PIN and D-PIN.

linewidths tend to overdamp toward the Γ point. This is reminiscent of the “waterfall,” as was discussed in Refs. 9, 26, and 36.

One of the most characteristic anomalies seen in the lead-based relaxor is waterfall;²⁶ the lowest-lying TO branch appears to precipitously drop into the acoustic branch at a finite value of the momentum transfer near $\delta=0.15$. The waterfall is widely seen in conventional relaxors such as PMN,⁹ PZN,³⁶ and their solid solutions with PT, PMN-*x*%PT,³⁷ and PZN-*x*%PT.²⁶ At the beginning of the finding of the waterfall, it was discussed in connection with PNR. However, it has been gradually understood that the waterfall is not directly related to the relaxor state because the waterfall behavior was observed even in the ferroelectric PZN-15%PT³⁸ and PMN-60%PT,³⁹ where PNR does not exist.

We speculate that the overdamping trend toward the Γ point, as seen in Fig. 6, is a waterfall-like anomaly. The results are consistent with the waterfall being unrelated to the PNR generation because the present waterfall-like behavior was seen in antiferroelectric O-PIN, where PNR is absent. The waterfall-like behavior is commonly seen in both O-PIN and D-PIN and is independent of the B-site randomness and PNR. As the waterfall does not appear in PT,⁴⁰ which has no A-site off-centerness,^{31–33} we suggest that the A-site off-centerness should play an important role in the appearance of the waterfall. We note again that the local environment of O-PIN is quite similar to that of D-PIN,²⁹ i.e., the lead ions are strongly off-center.

V. CONCLUSION

We studied the lattice dynamics of the PIN by high resolution IXS, taking much into account of the difference of the

B-site randomness, using O-PIN (AFE) and D-PIN (relaxor) single crystals. It has been found that there is a clear softening of TO mode at the Γ point in both samples, indicating a robust and intrinsic ferroelectric dynamical correlation regardless of the actual ground state. We believe that the correlation results in a FE instability mode, which gives yield to the FE and relaxor states. We now interpret that AFE is stabilized when In and Nb ions are spatially ordered, overwhelming the FE instability, and that the hidden FE state starts to appear as the B-site randomness becomes stronger and suppresses AFE instability. Ultimately, the randomness competes with the development of FE regions and blocks a long range FE order, which yields PNRs resulting in relaxor behaviors.

Finally, we have speculated that the B-site randomness suppresses the AFE instability and relatively enhances the FE instability, while it blocks a long range FE order. We have further supposed, in connection with the A-site off-centerness, that several kinds of instabilities coexist in the lead-based perovskite relaxors. The B-site randomness con-

trols a balance among several kinds of instabilities and finally chooses the FE instability but blocks a long range FE order.

The waterfall-like behavior was seen in both the samples. The results are consistent with the waterfall being unrelated to the PNR generation. Relation between the waterfall and the A-site off-centerness is also discussed.

ACKNOWLEDGMENTS

We would like to thank Y. Uesu, M. Iwata, Y. Fujii, and G. Shirane for stimulating discussions and ideas. We give special thanks to T. Mori for his valuable discussions. The high resolution inelastic x-ray scattering experiments were performed at SPring-8 with the approval of the Japan Synchrotron Radiation Research Institute (JASRI) (Proposal No. 2006B1311). This work was supported by Grant-in-Aid for Scientific Research on Priority Areas "Novel States of Matter Induced by Frustration" (Grant No. 19052002).

*ohwada@spring8.or.jp

- ¹G. A. Smolenskii and A. I. Agronovskaya, *Sov. Phys. Tech. Phys.* **A3**, 1380 (1958).
- ²G. A. Smolenskii, V. A. Isupov, A. I. Agronovskaya, and S. N. Popov, *Fiz. Tverd. Tela (Leningrad)* **2**, 2906 (1960), [*Sov. Phys. Solid State* **2**, 2584 (1961)].
- ³G. A. Smolenskii, A. I. Agronovskaya, and S. N. Popov, *Sov. Phys. Solid State* **2**, 2584 (1961).
- ⁴A. A. Bokov, I. P. Raevskii, O. I. Prokopalo, E. G. Fesenko, and V. G. Smotrakov, *Ferroelectrics* **54**, 241 (1984).
- ⁵N. Yasuda, H. Ohwa, J. Oohashi, K. Nomura, H. Terauchi, M. Iwata, and Y. Ishibashi, *J. Phys. Soc. Jpn.* **67**, 3952 (1998).
- ⁶H. Ohwa, M. Iwata, H. Orihara, N. Yasuda, and Y. Ishibashi, *J. Phys. Soc. Jpn.* **69**, 1533 (2000).
- ⁷G. Burns and F. H. Dacol, *Solid State Commun.* **48**, 853 (1983).
- ⁸G. Burns and F. H. Dacol, *Phys. Rev. B* **28**, 2527 (1983).
- ⁹P. M. Gehring, S. Wakimoto, Z.-G. Ye, and G. Shirane, *Phys. Rev. Lett.* **87**, 277601 (2001).
- ¹⁰S. Wakimoto, C. Stock, R. J. Birgeneau, Z.-G. Ye, W. Chen, W. J. L. Buyers, P. M. Gehring, and G. Shirane, *Phys. Rev. B* **65**, 172105 (2002).
- ¹¹S. B. Vakhrušev, A. A. Naberezhnov, N. M. Okuneva, and B. N. Savenko, *Fiz. Tverd. Tela (S.-Peterburg)* **37**, 3621 (1995), [*Phys. Solid State* **37**, 1993 (1995)].
- ¹²A. Naberezhnov, S. Vakhrušev, B. Dorner, D. Strauch, and H. Moudden, *Eur. Phys. J. B* **11**, 13 (1999).
- ¹³K. Hirota, Z.-G. Ye, S. Wakimoto, P. M. Gehring, and G. Shirane, *Phys. Rev. B* **65**, 104105 (2002).
- ¹⁴S. Wakimoto, C. Stock, Z.-G. Ye, W. Chen, P. M. Gehring, and G. Shirane, *Phys. Rev. B* **66**, 224102 (2002).
- ¹⁵J. Hlinka, S. Kamba, J. Petzelt, J. Kulda, C. A. Randall, and S. J. Zhang, *Phys. Rev. Lett.* **91**, 107602 (2003).
- ¹⁶C. Stock, H. Luo, D. Viehland, J. F. Li, I. P. Swainson, R. J. Birgeneau, and G. Shirane, *J. Phys. Soc. Jpn.* **74**, 3002 (2005).
- ¹⁷S. N. Gvasaliya, B. Roessli, R. A. Cowley, P. Huber, and S. G. Lushnikov, *J. Phys.: Condens. Matter* **17**, 4343 (2005).
- ¹⁸K. Ohwada, K. Hirota, H. Terauchi, H. Ohwa, and N. Yasuda, *J. Phys. Soc. Jpn.* **75**, 024606 (2006).
- ¹⁹G. Xu, H. Hiraka, G. Shirane, and K. Ohwada, *Appl. Phys. Lett.* **84**, 3975 (2004).
- ²⁰K. Nomura, N. Yasuda, H. Ohwa, and H. Terauchi, *J. Phys. Soc. Jpn.* **66**, 1856 (1997).
- ²¹K. Nomura, T. Shingai, S. Ishino, H. Terauchi, N. Yasuda, and H. Ohwa, *J. Phys. Soc. Jpn.* **68**, 39 (1999).
- ²²A. Q. R. Baron, Y. Tanaka, S. Goto, K. Takeshita, T. Matsushita, and T. Ishikawa, *J. Phys. Chem. Solids* **61**, 461 (2000).
- ²³A. Q. R. Baron, J. P. Sutter, S. Tsutsui, H. Uchiyama, T. Masui, S. Tajima, R. Heid, and K.-P. Bohnen, *J. Phys. Chem. Solids* (to be published).
- ²⁴B. Fak and B. Dorner, *Institute Laue Langevin Report No. 92FA008S*, 1992.
- ²⁵B. Dorner, *Coherent Inelastic Neutron Scattering in Lattice Dynamics*, Springer Tracts in Modern Physics Vol. 93 (Springer-Verlag, Berlin, 1982), p. 17.
- ²⁶P. M. Gehring, S.-E. Park, and G. Shirane, *Phys. Rev. Lett.* **84**, 5216 (2000).
- ²⁷Y. Uesu, H. Tazawa, K. Fujishiro, and Y. Yamada, *J. Korean Phys. Soc.* **29**, S703 (1996).
- ²⁸Y. Terado, S. J. Kim, C. Moriyoshi, Y. Kuroiwa, M. Iwata, and M. Takata, *Jpn. J. Appl. Phys., Part 1* **45**, 7552 (2006).
- ²⁹Y. Yoneda, K. Suzuya, J. Mizuki, and S. Kohara, *J. Appl. Phys.* **100**, 093521 (2006).
- ³⁰S. G. Zhukov, A. V. Yatsenko, and S. B. Vakhrušev, *J. Struct. Chem.* **38**, 486 (1997).
- ³¹S. Aoyagi, Y. Kuroiwa, A. Sawada, H. Tanaka, J. Harada, E. Nishibori, M. Takata, and M. Sakata, *J. Phys. Soc. Jpn.* **71**, 2353 (2002).
- ³²Y. Kuroiwa, H. Fujiwara, A. Sawada, S. Aoyagi, E. Nishibori, M. Sakata, M. Takata, H. Kawaji, and T. Atake, *Jpn. J. Appl. Phys., Part 1* **43**, 6799 (2004).

- ³³Y. Kuroiwa, S. Aoyagi, A. Sawada, J. Harada, E. Nishibori, M. Takata, and M. Sakata, *Phys. Rev. Lett.* **87**, 217601 (2001).
- ³⁴T. Shishidou, N. Mikano, Y. Uratani, F. Ishii, and T. Oguchi, *J. Phys.: Condens. Matter* **16**, S5677 (2004).
- ³⁵P. Ghosez, E. Cockayne, U. V. Waghmare, and K. M. Rabe, *Phys. Rev. B* **60**, 836 (1999).
- ³⁶P. M. Gehring, S.-E. Park, and G. Shirane, *Phys. Rev. B* **63**, 224109 (2001).
- ³⁷T. Y. Koo, P. M. Gehring, G. Shirane, V. Kiryukhin, S.-G. Lee, and S.-W. Cheong, *Phys. Rev. B* **65**, 144113 (2002).
- ³⁸D. La-Orautapong, B. Noheda, Z.-G. Ye, P. M. Gehring, J. Toulouse, D. E. Cox, and G. Shirane, *Phys. Rev. B* **65**, 144101 (2002).
- ³⁹C. Stock, D. Ellis, I. P. Swainson, Guanyong Xu, H. Hiraka, Z. Zhong, H. Luo, X. Zhao, D. Viehland, R. J. Birgeneau, and G. Shirane, *Phys. Rev. B* **73**, 064107 (2006).
- ⁴⁰G. Shirane, J. D. Axe, J. Harada, and J. P. Remeika, *Phys. Rev. B* **2**, 155 (1970).